Divalent cations potentiate TRPV1 channel by lowering the heat activation threshold

Xu Cao,[1,2] Linlin Ma,[2,3] Fan Yang,[2] KeWei Wang,[1,4] and Jie Zheng[2]

[1]Department of Molecular and Cellular Pharmacology, State Key Laboratory of Natural and Biomimetic Drugs, Peking University School of Pharmaceutical Sciences, Beijing 100191, China
[2]Department of Physiology and Membrane Biology, University of California School of Medicine, Davis, Davis, CA 95616
[3]Institute for Molecular Bioscience, The University of Queensland, Brisbane, St Lucia QLD 4072, Australia
[4]IDG/McGovern Institute for Brain Research, Peking University, Beijing 100871, China

Transient receptor potential vanilloid type 1 (TRPV1) channel responds to a wide spectrum of physical and chemical stimuli. In doing so, it serves as a polymodal cellular sensor for temperature change and pain. Many chemicals are known to strongly potentiate TRPV1 activation, though how this is achieved remains unclear. In this study we investigated the molecular mechanism underlying the gating effects of divalent cations Mg^{2+} and Ba^{2+}. Using a combination of fluorescence imaging and patch-clamp analysis, we found that these cations potentiate TRPV1 gating by most likely promoting the heat activation process. Mg^{2+} substantially lowers the activation threshold temperature; as a result, a significant fraction of channels are heat-activated at room temperature. Although Mg^{2+} also potentiates capsaicin- and voltage-dependent activation, these processes were found either to be not required (in the case of capsaicin) or insufficient (in the case of voltage) to mediate the activating effect. In support of a selective effect on heat activation, Mg^{2+} and Ba^{2+} cause a Ca^{2+}-independent desensitization that specifically prevents heat-induced channel activation but does not prevent capsaicin-induced activation. These results can be satisfactorily explained within an allosteric gating framework in which divalent cations strongly promote the heat-dependent conformational change or its coupling to channel activation, which is further coupled to the voltage- and capsaicin-dependent processes.

The Journal of General Physiology

INTRODUCTION

Transient receptor potential vanilloid type 1 (TRPV1) is a heat- and ligand-sensitive ion channel that is activated when the temperature reaches ~40°C at resting membrane potential or when capsaicin is present at 100 nM or higher concentrations (Caterina et al., 1997). The dual activation by heat and capsaicin provides a molecular explanation for the hot sensation elicited by chili peppers as well as the potential physiological role TRPV1 plays in sensing temperature change and pain. In addition, activity of TRPV1 is regulated by physical stimuli including voltage and mechanical force as well as a plethora of chemicals such as extracellular H^+, intracellular Ca^{2+}, and PIP_2 (Tominaga et al., 1998; Jordt et al., 2000; Chuang et al., 2001; Voets et al., 2004; Stein et al., 2006; Lukacs et al., 2007; Dhaka et al., 2009; Ufret-Vincenty et al., 2011; Cao et al., 2013). Sensitivity to a wide spectrum of stimuli allows TRPV1 to serve as a polymodal cellular sensor (Clapham, 2003; Zheng, 2013). Understanding how TRPV1 senses these stimuli is of great practical importance, as the channel is considered to be an attractive drug target for pain medication (Wu et al., 2010).

Like voltage-gated potassium channels, TRPV1 is a tetrameric protein complex with a centrally located ion permeation pore surrounded by channel subunits that contain six transmembrane segments and intracellularly located amino and carboxyl termini (Jahnel et al., 2001; Kedei et al., 2001; Kuzhikandathil et al., 2001; Moiseenkova-Bell et al., 2008). Chemical activators of TRPV1 are known to interact with many different channel structures. Capsaicin, for example, interacts with residues in the S2-to-S3 region, including likely π–π interactions between the vanillyl moiety of capsaicin and the aromatic ring of amino acids Y511 and/or F512 (of rat TRPV1; Jordt and Julius, 2002). Ca^{2+}-calmodulin binds to two potential intracellular binding sites, located in the C-terminal region and the N-terminal Ankyrin-like repeat domain (Lishko et al., 2007; Lau et al., 2012). Extracellular H^+ is found to bind to sites clustered at the outer pore region, mainly two glutamates (E600 and E648 in rat TRPV1; Jordt et al., 2000). The wide spread of chemical interaction sites suggests that an allosteric mechanism may underlie the integration of multiple TRPV1 stimuli in promoting channel activation. Gating

Correspondence to Jie Zheng: jzheng@ucdavis.edu; or KeWei Wang: wangkw@bjmu.edu.cn

Abbreviations used in this paper: ECS, extracellular solution; eYFP, enhanced YFP.

The Rockefeller University Press $30.00
J. Gen. Physiol. Vol. 143 No. 1 75–90
www.jgp.org/cgi/doi/10.1085/jgp.201311025

models incorporating allosteric mechanisms indeed have been proven to be successful in describing many aspects of TRPV1 gating (Latorre et al., 2007; Matta and Ahern, 2007; Jara-Oseguera and Islas, 2013).

In contrast to the detailed understanding of chemical activation of TRPV1, the molecular mechanisms governing the channel's response to most physical stimuli remain unclear. In particular, the heat activation process that underlines the role of TRPV1 as a heat and pain sensor is highly controversial. An important factor impeding research in this area is the lack of effective methods to pinpoint the sites affected by heat. It is well known that structural perturbations by mutation (deletion, chimera, etc.) of selected channel regions do not have only localized effects. Furthermore, unlike chemical stimuli that target specific protein sites, stimulus from heat is difficult to restrict to a specific protein site or region. When temperature rises, heat affects the whole protein as well as its surrounding lipids and the aqueous environment. As channel activity can be potentially affected by each of these components, it is difficult to distinguish what changes drive channel activation.

Given the available knowledge on the action sites and molecular mechanisms for TRPV1 chemical stimuli, it would be informative to know how chemical stimuli interact with the physical stimuli of TRPV1, especially if such interaction is specific. Results from our recent studies (Yang et al., 2010; Cui et al., 2012) and other studies (Matta and Ahern, 2007; Grandl et al., 2010) revealed that capsaicin and heat apparently activate TRPV1 through separate pathways. In this paper, we investigated the gating mechanism of another type of chemical stimuli for TRPV1, the divalent cations. Divalent and multivalent cations such as Mg^{2+}, Ni^{2+}, Gd^{3+}, and polyamines are potent TRPV1 activators (Ahern et al., 2005, 2006; Tousova et al., 2005; Riera et al., 2007; Ohta et al., 2008; Luebbert et al., 2010). Divalent cations have simple chemistry, high water solubility, and low membrane permeability (in contrast to, for example, capsaicin), and are chemically inert. These preferable features make divalent cations an attractive tool for the investigation of the TRPV1 gating mechanism. For these reasons, in this paper and the accompanying paper (see Yang et al. in this issue) we examined the mechanism and structural determinants of TRPV1 potentiation by two divalent cations, Mg^{2+} and Ba^{2+}.

The present study focused on the activation mechanism. We assessed the permeation effect of Mg^{2+}, the concentration dependence in promoting channel activation, and the channel open probability that could be reached by Mg^{2+} stimulation. We then quantified and compared the energetic effects of Mg^{2+} on various TRPV1 activation pathways. Our observations showed that these cations strongly potentiate channel activation, which can be satisfactorily explained within an allosteric framework assuming that divalent cations directly potentiate the heat-activation pathway, but cannot be easily explained if instead their gating effects are assumed to originate from potentiating the voltage- or capsaicin-activation pathways. In support of a specific effect on heat activation, we observed that prolonged application of Mg^{2+} and Ba^{2+} selectively desensitizes heat activation while sparing capsaicin activation. These results identify divalent cations as a distinct group of TRPV1 agonists. In addition, they further support the notion that heat and capsaicin activate TRPV1 through different pathways (Jordt et al., 2000; Matta and Ahern, 2007; Yang et al., 2010; Cui et al., 2012). Our findings demonstrate that divalent cations can be a useful tool in the search for the heat activation mechanism. In Yang et al. (2014), we describe experiments aimed at identifying channel structures that mediate the gating effects of divalent cations.

MATERIALS AND METHODS

cDNA constructs and cell transfection

The mouse TRPV1 (a gift from M.X. Zhu, University of Texas Health Science Center at Houston, Houston, TX) was used in this study. This cDNA has 95% and 87% overall sequence identity to the rat and human TRPV1 cDNAs, respectively. Functional properties of mTRPV1 are also very similar to rTRPV1 and hTRPV1, on which several previous studies on the gating effects of cationic ions were performed. To facilitate identification of channel-expressing cells, the cDNA encoding enhanced YFP (eYFP) was fused in frame to the C-terminal end of the mTRPV1 cDNA, as described previously (Cheng et al., 2007).

HEK293 cells were cultured in a DMEM medium supplemented with 10% FBS, 100 U/ml penicillin, and 100 mg/ml streptomycin at 37°C with 5% CO_2. Cells were passaged 6–24 h before transfection by plating onto glass coverslips coated with 0.1 mg/ml poly-L-lysine to improve cell adhesion and subsequent patch recordings. Transient transfection was conducted by adding 4 µg plasmid DNA and 4 µl Lipofectamine 2000 (Invitrogen) in a 6-well plate. Electrophysiological experiments and fluorescence imaging recordings were performed between 24 h and 48 h after transfection.

Electrophysiological recordings

Macroscopic and single-channel currents were recorded from TRPV1-expressing cells using a HEKA EPC10 amplifier controlled with PatchMaster software (HEKA). Patch pipettes were pulled from borosilicate glass and fire-polished to a resistance of ~2 MΩ. Membrane potential was held at 0 mV and, unless otherwise stated, currents were elicited by a protocol consisting of a 300-ms step to +80 mV followed by a 300-ms step to −80 mV at 1-s intervals. Data were filtered at 2.25 kHz and sampled at 12.5 kHz. As TRPV1 macroscopic current was strongly outward-rectifying mainly due to rapid deactivation at −80 mV, current amplitude was analyzed at +80 mV. Both whole-cell and inside-out configurations were used in this study, while Mg^{2+} or Ba^{2+} were always added to the extracellular solution. During whole-cell recordings the capacitance current was minimized by amplifier circuitry. The series resistance (typically 5–20 MΩ) was compensated by 80%; after compensation the voltage errors should be <5 mV. The standard bath solution and pipette solution contained 130 mM NaCl and 3 mM Hepes, pH 7.2. Mg^{2+} or Ba^{2+} solution contained 130 mM $MgCl_2$ or $BaCl_2$, and 3 mM Hepes, pH 7.2. Solutions containing 10–100 mM Mg^{2+} were prepared from the 130 mM Mg^{2+}–containing solution by replacing the appropriate concentration of $MgCl_2$

with NaCl. Solution switching was achieved with a rapid solution changer RSC-200 (Bio-Logic USA).

Temperature control and monitoring

The bath solution was heated using an SHM-828 eight-line heater driven by a CL-100 temperature controller (Harvard Apparatus). To obtain a complete temperature–current relationship, in some experiments the bath solution was first cooled by embedding the perfusion solution reservoir in ice water. We placed a TA-29 miniature bead thermistor (Harvard Apparatus) ~1 mm from the pipette tip to monitor local temperature change. Temperature readout from the thermistor was fed into an analogue input port of the patch-clamp amplifier and recorded simultaneously with channel current. The speed of temperature change was set at a moderate rate of ~0.3°C/s to ensure that heat activation reached equilibrium during the course of temperature change and the current was recorded at steady-state. When the experimental temperature was not controlled, recordings were conducted at room temperature at 24°C.

Using fluorescence imaging to record TRPV1 activity

To monitor TRPV1 activity in intact living cells, we chose to use the high-affinity calcium indicator Fluo-4 (K_d for Ca^{2+} is 345 nM), which yields a large fluorescence intensity increase upon Ca^{2+} binding and its excitation spectrum, peaking at 494 nm, and is compatible with an argon laser (Gee et al., 2000). As a divalent cation chelator, Fluo-4 may potentially also bind Mg^{2+}, especially as in our experiments concentrations up to 130 mM (comparing to 1.8 mM Ca^{2+}) were applied to cells expressing TRPV1, a nonselective cation channel. Although there is no report available on the binding affinity of Mg^{2+} to Fluo-4, Mg^{2+} binds to the closely related Ca^{2+} indicator dye Fluo-3 with an extremely low affinity (K_d of 9 mM; Minta et al., 1989). This low binding affinity, in combination with the observation that binding of Mg^{2+} to Fluo-3 increases fluorescence weakly (only 1.4-fold, comparing to a 40-fold increase by Ca^{2+} binding), suggests that in our experiments the fluorescence signal came predominantly from binding of Ca^{2+} that entered the cell through open TRPV1 channels, whereas Mg^{2+} might also contribute to the total fluorescence change. This prediction was confirmed experimentally. As shown in Fig. S1, in the absence of Ca^{2+}, Mg^{2+} was indeed able to yield small fluorescence signals when entering the cell, but only <10% in amplitude comparing to the signal generated by Ca^{2+}. Control experiments using cells pretreated with thapsigargin (1 µM), an inhibitor for sarcoplasmic reticulum Ca^{2+} ATPase (SERCA pump), did not exhibit a noticeable difference in fluorescence signal intensity or kinetics compared with untreated cells. This observation further confirmed that changes in fluorescence intensity were caused by Ca^{2+} entry upon heat, capsaicin, or Mg^{2+} stimuli, instead of the release of Ca^{2+} from the intracellular store.

For fluorescence imaging experiments, TRPV1-expressing HEK293 cells seeded on 25-mm coverslips were subjected to imaging 24–48 h after transfection. After washing once with an extracellular solution (ECS) containing 140 mM NaCl, 5 mM KCl, 1 mM $MgCl_2$, 1.8 mM $CaCl_2$, 10 mM glucose, and 15 mM HEPES, pH 7.4, cells were incubated in 2 ml of ECS supplemented with 2 µM fluo-4/AM and 0.1% Pluronic F-127 (both from Invitrogen) at room temperature for 60 min. 2 mM Probenecid (Invitrogen) was included in all solutions during imaging to prevent fluo-4 leakage from loaded cells. After incubation, cells were washed three times with ECS and incubated in the same solution for another 20 min to complete the intracellular hydrolysis process of the AM ester, which converts the nonfluorescent Fluo-4/AM into the fluorescent Fluo-4.

Coverslips with dye-loaded cells were placed in the quick-release magnetic chamber (Warner Instruments) and mounted on the stage of a microscope system (Eclipse TE2000-U; Nikon) equipped with a CCD camera (Cascade 128B; Roper Scientific). Fluo-4 was excited by an Argon laser with a filter set of Z488/10 (excitation), z488rdc (dichroic) and recorded through an emission filter HQ500lp (all from Chroma Technology Corp.). The same excitation intensity was used for all the experiments. The duration of light exposure was controlled by a computer-driven mechanical shutter (Uniblitz). Cell images were acquired sequentially with an exposure period of 200 ms at an interval of 1 s. Both the shutter and the camera were controlled with MetaMorph software (Universal Imaging).

ECS with varying concentration of Mg^{2+} was delivered right next to the imaging area by an RSC-200 rapid solution-switching system through separate lines. Temperature control during imaging was achieved by perfusing preheated solutions in the same way as for electrophysiology studies. A TA-29 miniature bead thermistor (Harvard Apparatus) was placed right next to the imaging area to ensure accurate monitoring of local temperature. The thermistor's temperature readout was fed into an analogue input of the patch amplifier; MetaMorph software was synchronized with PatchMaster software to record temperature simultaneously with imaging. All experiments except heat activation studies were performed at room temperature.

For imaging data processing, the cell boundary was defined manually in MetaMorph. The boundary defined individual regions of interest (ROIs). The mean fluorescence intensity of each ROI was measured and exported to Excel (Microsoft). When an equilibrium state was reached after application of a stimulus, the mean fluorescence intensity, F, of all pixels within each ROI was calculated. Changes in fluorescence intensity, ΔF, were calculated as the difference between the equilibrium level after stimulus application and the baseline. By measuring fluorescence changes, background fluorescence from eYFP and scatter light were excluded. The background fluorescence was not affected by Mg^{2+} under our experimental conditions.

Data analysis

We used the current–temperature relationship to determine activation threshold temperature and to characterize thermodynamic properties of heat activation (Cui et al., 2012). The raising phase of the current–temperature curve recorded from cells expressing wild-type or mutant TRPV1 channels showed two temperature-dependent phases: a less temperature-dependent phase at lower temperatures followed by a higher temperature-dependent phase at higher temperatures. We fitted each phase to a linear function. The temperature at the intersection of the two lines was defined as the activation threshold temperature. The same approach was used to estimate the activation threshold from fluorescence imaging data.

To calculate the enthalpic change, ΔH, and the entropic change, ΔS, associated with heat activation, we chose the high temperature–dependent phase to construct a Van't Hoff plot and fitted it to the following equation:

$$\ln K_{eq} = -\frac{\Delta H}{RT} + \frac{\Delta S}{R},$$

where K_{eq} is the equilibrium constant calculated from the channel open probability, R is the gas constant, and T is the temperature in Kelvin. Because the single-channel conductance is temperature dependent, the macroscopic current amplitudes at different temperatures were corrected by converting them to a level as if the temperature were 20°C (Yang et al., 2010). The open probability was determined as the ratio between the macroscopic current (after correcting for temperature-dependent single-channel conductance) and the maximum current estimated using noise analysis (Sigworth, 1980). The mean current amplitude, I, and the corresponding variance, σ^2, were estimated from the plateau

phase of each sweep. Noise analysis was then applied to estimate the number of channels and the maximum current level, using the following equation $\sigma^2 = iI - I^2/N$, in which i is the single-channel amplitude and N is the number of channels. The half-activation temperature, T_{half}, at which the heat activation is 50% complete, was calculated as $T_{half} = \Delta H/\Delta S$.

G-V curves were fitted to a single-Boltzmann function:

$$\frac{G}{G_{max}} = \frac{1}{1 + e^{-\frac{qF}{RT}(V - V_{half})}}, \quad (1)$$

where G/G_{max} is the normalized conductance estimated from the steady-state current at each testing voltage, q is the equivalent gating charge, V_{half} is the half-activation voltage, and F is Faraday's constant.

The capsaicin dose–response relationship was fitted with the Hill equation:

$$\frac{I_x - I_{min}}{I_{max}} = \frac{[x]^n}{EC_{50}^n + [x]^n},$$

where I_x is the steady-state TRPV1 current in the presence of capsaicin at concentration $[x]$, I_{min} and I_{max} are the current amplitude in the absence and the presence of a saturating concentration of capsaicin, respectively, EC_{50} is the capsaicin concentration at which activation is half-maximal, and n is the slope factor.

Single-channel conductance was estimated from all-point histograms constructed from current events recorded at +80 mV. A double-Gaussian function was fitted to the histograms. From the positions of the Gaussian peaks the closed and open current levels were identified, and single-channel current amplitude and the corresponding conductance were calculated.

All values are given as mean ± SEM for the number of measurements indicated (n). Statistical significance was determined using the Student's t test, and indicated as follows: *, $P < 0.05$; **, $P < 0.01$; ***, $P < 0.001$.

Multi-allosteric gating model

The approach we used for the study of the TRPV1 polymodal gating was inspired by the work on Ca^{2+}-sensitive voltage-gated BK channels by Aldrich, Horrigan, and Cui (Horrigan and Aldrich, 1999, 2002; Horrigan et al., 1999). Using a structure-independent, dual-allosteric gating model, these authors demonstrated nicely that near-independent gating transitions caused by Ca^{2+} binding and voltage sensor movement exert substantial influence on each other through their convergence onto the channel opening transition. Similarly, our approach to a general gating model for TRPV1 assumed that the closed-to-open transition, C↔O, and the transition induced by a given activation stimulus, R↔A, are both reversible transitions that are coupled allosterically (Scheme I in Fig. 1). In this case, the channel open probability, P_o, is determined by the equilibrium constants of the two transitions, L and D, as well as the allosteric coupling factor between the two transitions, J, according to the following equation:

$$P_o = \frac{L(1 + JD)}{L(1 + JD) + (1 + D)}, \quad (2)$$

where $L = L_0 \exp(w_L/RT)$ and $D = D_0 \exp(w_D/RT)$. w_L and w_D are the free energy associated with the C↔O and R↔A transition, respectively. Through allosteric coupling factor J, the equilibrium constant D exerts its effect on the channel open probability, which is the experimentally observable parameter. For a strong coupling, $J \gg 1$, and P_o is strongly dependent on D. In the extreme case when $J = 1$, there is no coupling between the two transitions, and the open probability becomes independent of D: $P_0 = L/(1 + L)$.

Applying this general, structure-independent principle to the polymodal activation of TRPV1 by voltage, capsaicin, and heat yielded Scheme II (Fig. 1 B), in which the closed-to-open transition, C↔O, is allosterically coupled to the voltage-dependent transition between the resting state and the activated state, R↔A, the capsaicin-induced transition between the unliganded state and the liganded state, U↔L, and the heat-induced transition between the native state and the permissive state, N↔P, with a coupling factor of J_V, J_C, and J_H, respectively. When two instead of three activation stimuli are present simultaneously, Scheme II (Fig. 1 B) reduces to a dual-allosteric system equivalent to the one for the BK channel (Horrigan and Aldrich, 2002). Under conditions that prohibit all but one activation pathway, Scheme II reduces to Scheme I (Fig. 1), with the channel open probability determined by two equilibrium constants and one coupling factor as shown by Eq. 2. In support of the multi-allosteric gating model of Scheme II (Fig. 1 B), we and others have found that heat and capsaicin activate TRPV1 through separate pathways that are energetically coupled (Grandl et al., 2010; Yang et al., 2010; Cui et al., 2012). Similarly, voltage and capsaicin stimuli exhibit an additive effect on activation (Matta and Ahern, 2007; Yang et al., 2010). In principle, transitions induced by the three stimuli can also be allosterically coupled (as shown by the dashed lines in Fig. 1 B, Scheme II) with coupling factors J_{CH}, J_{CV}, and J_{VH}. Observations

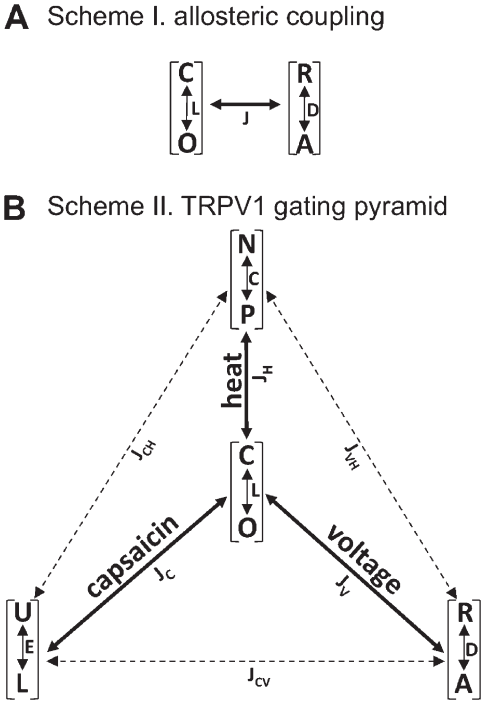

Figure 1. Allosteric gating schemes. (A) A general allosteric coupling system containing a reversible closed (C) to open (O) transition with an equilibrium constant L, a reversible transition between a relaxed state (R) and an activated state (A) with an equilibrium constant D, and a coupling factor J. The measurable parameter is the probability of being in the O state, which is determined by both the C↔O equilibrium and the R↔A equilibrium. No additional constraint is assumed in this structure-independent model. (B) A multi-allosteric model for the gating of TRPV1 by voltage, capsaicin, and heat, in which the C↔O equilibrium at the apex of the pyramid is coupled allosterically to each of the stimulus-induced transitions according to the general principle shown in Scheme I. Definition of states and coupling factors are given in Materials and methods.

from our previous experiments suggested that J_{CH} is apparently quite small (Cui et al., 2012). Nonetheless, in this study we did not attempt to estimate the strength of coupling between different stimuli. Likewise, we were not concerned with obtaining an accurate estimate of the coupling factors J_V, J_C, and J_H. Our focus was instead on estimating the energetic effect of divalent cation Mg^{2+} on each of the three branches of Scheme II (Fig. 1 B), from which we can gain insights into the mechanistic nature of Mg^{2+} potentiation of TRPV1. The energetic effect of 100 mM Mg^{2+} on the voltage-dependent activation was estimated from the shift of the *G-V* curve upon application of the divalent cation: $\Delta E_V = qF\Delta V$, in which ΔE_V is the free energy difference in voltage-dependent activation in the absence and presence of Mg^{2+}, q is the apparent gating charge, F is the Faraday's constant, and ΔV is the shift in half-activation voltage V_{half} (see Eq. 1). The energetic effect of 10 mM Mg^{2+} on the capsaicin-induced activation was estimated from the shift of the capsaicin dose–response curve: $\Delta E_C = nRTln(EC_{50}/EC'_{50})$, in which ΔE_C is the free energy difference in ligand activation caused by Mg^{2+}, EC_{50} and EC'_{50} are the half-activation concentrations of capsaicin in the absence and presence of Mg^{2+}, respectively, and n is the Hill slope factor. The energetic effect of 10 mM Mg^{2+} on heat-dependent activation was estimated from the change in the free energy associated with the heat activation process: $\Delta E_H = \Delta G_2 - \Delta G_1$, in which ΔE_H is the free energy difference in heat activation in the absence and presence of Mg^{2+}, ΔG_1, and ΔG_2. ΔG_1 and ΔG_2 were calculated from the enthalpy and entropy using the Gibbs equation $\Delta G = \Delta H - T\Delta S$ as described earlier.

Online supplemental material

Fig. S1 shows that fluorescence intensity increase upon channel opening was mainly induced by Ca^{2+}, whereas Mg^{2+} could also induce a small fluorescence signal. Fig. S2 shows that the representative time course of the temperature-dependent fluorescence intensity changes upon heating in a TRPV1-expressing cell. Online supplemental material is available at http://www.jgp.org/cgi/content/full/jgp.201311025/DC1.

RESULTS

Mg^{2+} induces influx of divalent cations in TRPV1-expressing HEK293 cells

We first examined the effect of Mg^{2+} on TRPV1 activation by recording intracellular fluorescence increase due to Ca^{2+} (and Mg^{2+}) influx through open channels. The mouse TRPV1 channel was expressed in HEK293 cells that were then loaded with the Ca^{2+} indicator dye Fluo-4. Introducing Mg^{2+} into the bath solution at room temperature induced a fluorescence signal in a dose-dependent manner (Fig. 2 A). Although 30 mM Mg^{2+} could induce a clearly observable increase in fluorescence intensity, further increasing the Mg^{2+} concentration to 100 mM significantly boosted the fluorescence signal, indicating that the apparent EC_{50} value must be >30 mM (Fig. 2, B and C). It is worth noting that this is at least three-to-four orders of magnitude higher than the EC_{50} value for capsaicin on mouse TRPV1, which we previously estimated to be 0.95 µM (Cui et al., 2012), as well as the EC_{50} value for proton, at ~10 µM, pH 5 (unpublished data). The Mg^{2+} sensitivity of mouse TRPV1 appeared to be slightly lower than that of human TRPV1 recorded with a different Ca^{2+} dye, Fura-2 (Riera et al., 2007). We noticed that, with 100 mM Mg^{2+}, the fluorescence intensity declined over time with a time constant of many seconds (see Fig. 2 B), which is correlated with a slow desensitization process (as described later). In summary, our results from intact live cells suggest that at millimolar concentrations, Mg^{2+} causes TRPV1 activation at room temperature, followed by slow desensitization.

Mg^{2+} strongly potentiates TRPV1 current

To directly observe Mg^{2+} effects on TRPV1 activation, we recorded TRPV1 currents using whole-cell patch clamp in the presence of various concentrations of Mg^{2+} in the bath. Channel-expressing cells were identified by the fluorescence signal from an eYFP tag at the channel's C-terminal end, which were confirmed by the elicitation of TRPV1-mediated currents by 3 µM capsaicin. In close agreement with previous reports on rat and human TRPV1 channels (Ahern et al., 2005; Wang et al., 2010), extracellular Mg^{2+} at 10–100 mM concentrations strongly potentiated TRPV1, eliciting noticeable currents at room temperature (Fig. 3 A).

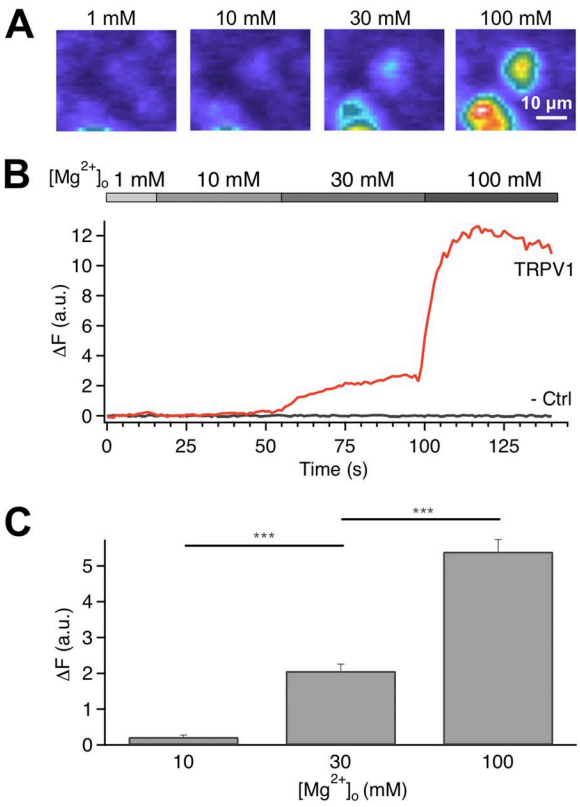

Figure 2. Mg^{2+} induces Ca^{2+} influx in TRPV1-expressing cells. (A) Live-cell fluorescence imaging of changes in intracellular Ca^{2+} concentration. (B) Representative time courses of the fluorescence signal in a channel-expressing cell and an untransfected cell. Changes in fluorescence intensity are shown in arbitrary units after subtracting the basal level intensity. (C) Change in fluorescence intensity increases with Mg^{2+} concentration. ***, $P < 0.001$; $n = 70–113$. Error bars indicate ±SEM.

Consistent with fluorescence imaging recordings, current induction by Mg^{2+} exhibited clear concentration dependence and did not show any sign of saturation at 100 mM. At this concentration, the Mg^{2+}-elicited current was ~15% in amplitude compared with that elicited by 3 µM capsaicin, a saturating concentration (Fig. 3 B, black bars).

Mg^{2+} reduces TRPV1 single-channel conductance

We conducted single-channel recording in the inside-out configuration, with various concentrations of Mg^{2+} in the pipette solution. We observed that extracellular Mg^{2+} clearly made the channel opening events longer and occur more frequently (Fig. 4 A), which is consistent with a potentiating effect on gating. In addition, Mg^{2+} dose-dependently inhibited the single-channel current amplitude (Fig. 4, A and B; Samways and Egan, 2011). In the Mg^{2+}-free solution, the single-channel conductance of TRPV1 outward current was estimated to be 133.8 ± 3.4 pS (n = 4), similar to that reported previously (Caterina et al., 1997; Premkumar and Ahern, 2000). At the 100-mM concentration, Mg^{2+} reduced single-channel conductance by 50%, to 66.5 ± 0.1 pS (n = 4; Fig. 4, B and C). Thus Mg^{2+} dose-dependently potentiates TRPV1 through a gating effect but at the same time inhibits conductance. The dual effect of Mg^{2+} on gating and permeation could be seen in a previous study in which Mg^{2+} potentiated human TRPV1 current elicited by capsaicin (which partially activated the channel) but inhibited rat TRPV1 current elicited by capsaicin (which fully activated the channel; Wang et al., 2010).

Estimation of the channel open probability induced by Mg^{2+}

As the permeation effect of Mg^{2+} would partially mask the gating effect, in order to estimate the open probability of TRPV1 in the presence of Mg^{2+} we used the Mg^{2+} concentration dependence in single-channel conductance to adjust the whole-cell current amplitudes. Removing the permeation effect revealed a larger gating effect by Mg^{2+}. We estimated that, at saturating capsaicin concentrations and +80 mV, the mouse TRPV1 activation reaches an open probability of ~80%. Based on the amplitude ratio between the adjusted Mg^{2+}-elicited current and the capsaicin-elicited current, 100 mM Mg^{2+} potentiated the channel to an open probability of ~25% (n = 5; Fig. 3 B, red bars). Our data thus demonstrated that Mg^{2+} is a strong activator for TRPV1.

Having established that Mg^{2+} directly and potently activates TRPV1, we focused our attention on the molecular mechanism underlying the Mg^{2+}-mediated activation process. Our approach was based on a general, structure-independent, multi-allosteric framework in which each of the major TRPV1 stimuli (capsaicin, voltage, and heat) promotes a transition in the channel that is allosterically coupled to the closed-to-open transition (Fig. 1 B). We wanted to test which activation pathway is predominantly affected by Mg^{2+}. For this purpose we designed experiments to examine the energetic effect of Mg^{2+} on each of the activation pathways.

Effects of Mg^{2+} on voltage-dependent activation

One potential mechanism for Mg^{2+} potentiation of TRPV1 gating is through shifting the voltage-dependent activation process. To investigate this possibility, we compared the voltage dependence of TRPV1 activation with and without extracellular Mg^{2+} (Fig. 5 A). At 100 mM, Mg^{2+} shifted the G-V curve by −46 mV without a significant change in the steepness (Fig. 5 B). The shift in V_{half} would make depolarization more effective in activating TRPV1. However, because TRPV1 is very weakly voltage-dependent, having an apparent gating charge of ~0.5 e_0 (Fig. 5 B; Voets et al., 2004; Matta and Ahern, 2007), it is unlikely that the Mg^{2+} potentiating effect is wholly caused by the shift in voltage dependence. Indeed, the shift in the G-V curve alone will increase the open probability at +80 mV by a mere 61% (Fig. 5 B), whereas based on the adjusted current amplitudes shown in Fig. 3 B, at +80 mV, 100 mM Mg^{2+} increased the open probability by 26-fold. From the shift of V_{half} and the overall voltage dependence of channel activation, it was estimated that the energetic effect of 100 mM Mg^{2+} on voltage-dependent activation is ~0.5 kcal/mol. (The effect of 10 mM Mg^{2+} would be too small to estimate accurately.)

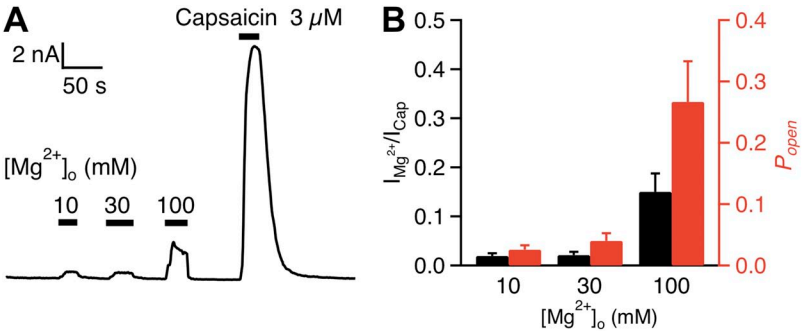

Figure 3. Mg^{2+} activates TRPV1 current in a dose-dependent manner. (A) Representative whole-cell currents at +80 mV evoked by Mg^{2+} and capsaicin. (B) Mean currents (black bars) evoked by Mg^{2+} normalized to the response evoked by 3 µM capsaicin (left axis). The red bars represent the same data after correction for Mg^{2+} inhibition of the single-channel conductance (see Fig. 4), so that the height of the bars directly reflects relative open probability (right axis). n = 5 each. Error bars indicate ±SEM.

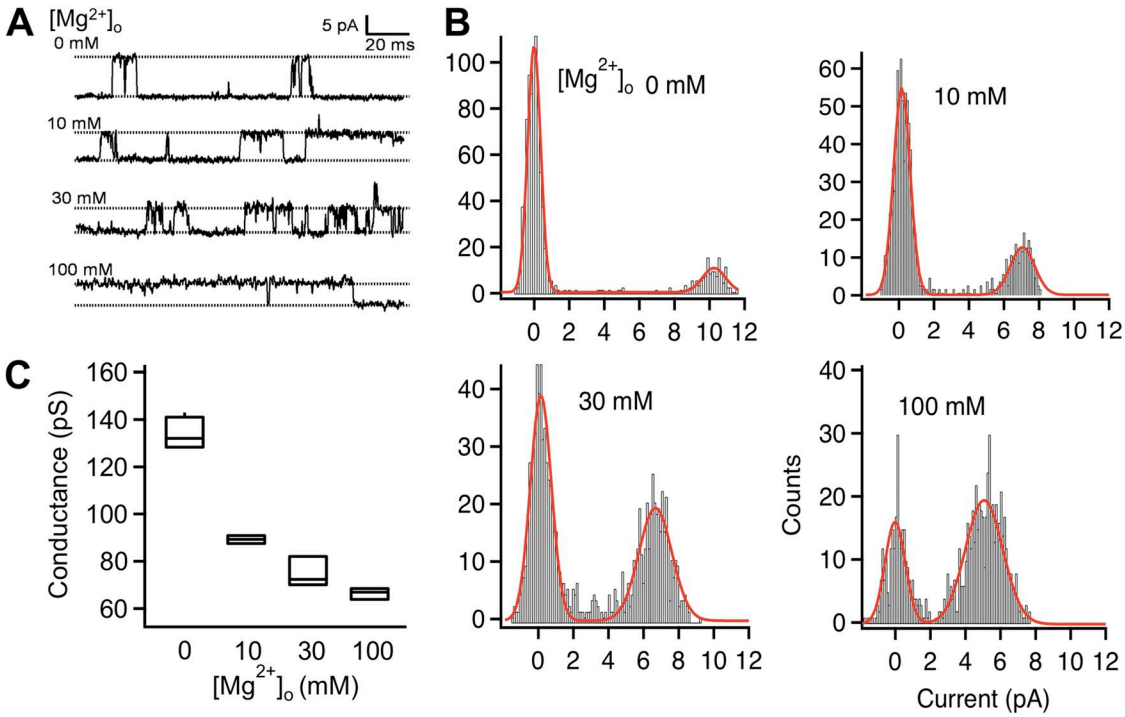

Figure 4. Mg^{2+} reduces the single-channel conductance of TRPV1. (A) Representative single-channel current traces recorded at +80 mV with the indicated concentrations of extracellular Mg^{2+}. (B) All-point histograms of single-channel events at the indicated Mg^{2+} concentrations. The superimposed curve represents a fit of a double-Gaussian function. (C) Box-and-whisker plot of the single-channel conductance versus the corresponding Mg^{2+} concentration. The whisker top, box top, line inside the box, box bottom, and whisker bottom represent the maximum, 75th percentile, median, 25th percentile, and minimum value of each pool of conductance measurements, respectively. n = 3–4.

Effects of Mg^{2+} on capsaicin activation

Potentiation of TRPV1 by Mg^{2+} does not require the presence of capsaicin. Nonetheless, Mg^{2+} and capsaicin do exhibit synergy in activating the channel so that in the presence of Mg^{2+}, capsaicin activation is more prominent (Ahern et al., 2005; Wang et al., 2010). We observed that Mg^{2+} shifted the capsaicin dose–response curve appreciably to the left (Fig. 6), which would make capsaicin a more potent agonist in the presence of Mg^{2+}. To further characterize interaction between Mg^{2+} and the capsaicin activation pathway, we estimated the energetic effect of Mg^{2+} on capsaicin activation from the Mg^{2+}-induced change in EC_{50}. As shown in Fig. 6, 10 mM Mg^{2+} shifted the EC_{50} value from 977 ± 15 nM (n = 3) to 282 ± 20 nM (n = 4) with a minor effect on the Hill slope factor (1.88 ± 0.05 and 1.61 ± 0.10, respectively; $P > 0.05$). The shift in EC_{50} value reflects a 1.2 kcal/mol energetic contribution to activation at room temperature.

Mg^{2+} substantially lowers the activation threshold temperature

We next examined the effect of Mg^{2+} on heat activation. Mg^{2+} of various concentrations was added to the pipette solution, and heat-induced TRPV1 activation was

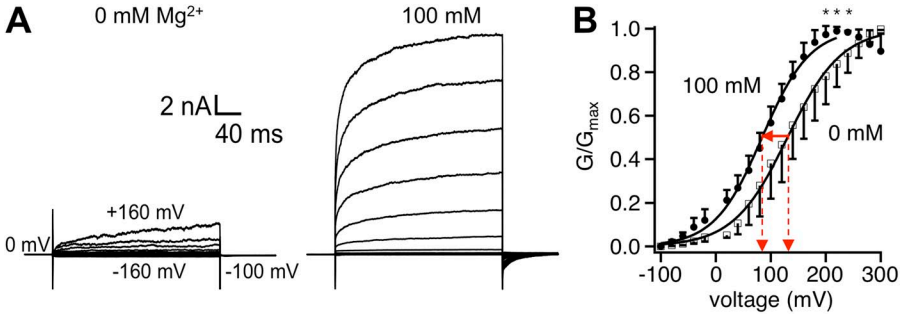

Figure 5. Effects of Mg^{2+} on the voltage-dependent activation of TRPV1. (A) Representative whole-cell patch-clamp current traces in response to a family of voltage steps in the absence (left) or presence (right) of 100 mM Mg^{2+}. Voltage steps were applied from a holding potential of 0 mV to various membrane potentials from −160 to +160 mV, in 20-mV steps. (B) G-V curves in the absence (open symbols) or presence (closed symbols) of 100 mM Mg^{2+} normalized to the respective G_{max} value. Superimposed are fits of a Boltzmann function with the following V_{half} and q values: 0 Mg^{2+}, 130.5 ± 1.6 mV, 0.53 ± 0.03 e_0 (n = 5); 100 mM Mg^{2+}, 84.3 ± 1.9 mV, 0.56 ± 0.06 e_0 (n = 5). Asterisks indicate a significant difference in the normalized conductance values ($P < 0.05$). Error bars indicate ±SEM.

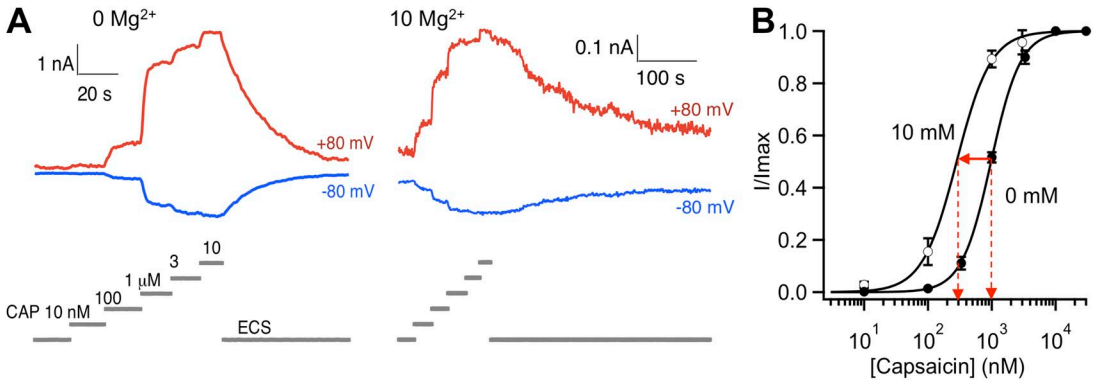

Figure 6. Effects of Mg^{2+} on the capsaicin-dependent activation of TRPV1. (A) Representative whole-cell current traces in response to varying capsaicin concentration in the absence (left) or presence (right) of 10 mM Mg^{2+}. (B) Dose-dependent activation of TRPV1 by capsaicin in the absence (closed circles) or presence (open circles) of 10 mM Mg^{2+}. Curves represent fits of a Hill equation. The EC_{50} and slope factor values are: 977 ± 15 nM and 1.88 ± 0.05 (n = 3) for 0 mM Mg^{2+}, and 282 ± 20 nM and 1.61 ± 0.10 (n = 4) for 10 mM Mg^{2+}. Error bars indicate ±SEM.

recorded from inside-out patches perfused by a heated solution. Heat-induced channel activation was monitored by the time course of current increase. Unlike a previous observation with rat TRPV1 in oocytes (Ahern et al., 2005), Mg^{2+} was found to substantially shift the temperature dependence of TRPV1 (Fig. 7, A and B). In the absence of divalent cation, TRPV1 activated at 37.7 ± 0.3°C (n = 9; Fig. 7, B and C). With 10 mM Mg^{2+}, the threshold temperature was significantly lowered to 30.2 ± 1.1°C (n = 8, P < 0.001). Increasing the Mg^{2+} concentration to 30 mM further shifted the threshold temperature to 20.2 ± 1.8°C (n = 8, P < 0.001) so that even at room temperature TRPV1 was open at an appreciable level (Fig. 7 C). The large shift in threshold temperature made it impractical to further increase Mg^{2+} concentration for these experiments. Nonetheless, it is clear that Mg^{2+} has a strong effect on heat activation.

Fluorescence imaging experiments confirmed that Mg^{2+} substantially affected the heat response of TRPV1. While raising temperature in the presence of 1 mM Mg^{2+} (the control solution) caused a gradual increase in the fluorescence signal, the same manipulation in the presence of 10 mM Mg^{2+} elevated the fluorescence signal to a higher level more rapidly and at lower temperatures (Fig. 8 A; see also Fig. S2). With 10 mM Mg^{2+}, the peak fluorescence intensity was more than doubled (Fig. 8 B), whereas the mean activation threshold temperature for fluorescence increase was shifted by ~6°C (Fig. 8 C). These results from live cells again suggest that further increases in the Mg^{2+} concentration would

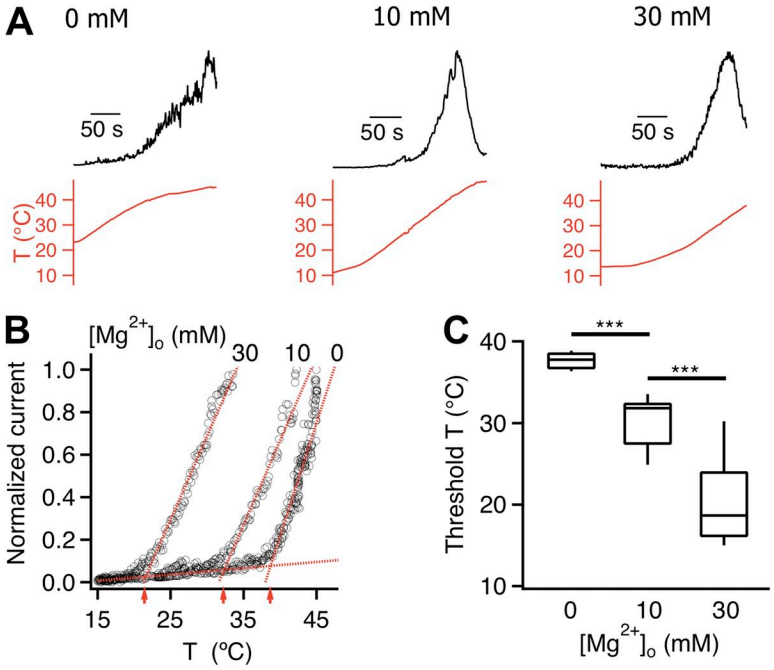

Figure 7. Mg^{2+} strongly potentiates the temperature response of TRPV1. (A) Normalized current (top) induced by a temperature ramp (bottom) recorded from inside-out patches at +80 mV with 0 mM, 10 mM, and 30 mM Mg^{2+} in the pipette solution. Recordings are from three separate patches. (B) The current raising phase is shown as a function of temperature. The activation threshold temperatures, at the intersection of a pair of dotted lines (representing the leak current and the heat-activated TRPV1 current), are indicated by red arrows. (C) Mg^{2+} dose-dependently lowered the activation temperature. ***, P < 0.001; n = 8–9.

cause an increasing fraction of TRPV1 channels to be heat-activated at room temperature.

We characterized the energetic effect of Mg^{2+} on heat activation with thermodynamic analysis. It is well established that large changes in enthalpy and entropy are hallmarks of the highly temperature-sensitive heat activation process of TRPV1 and other thermo-TRP channels (Voets et al., 2004; Yang et al., 2010; Yao et al., 2010). Reflecting a large energetic effect by Mg^{2+} on heat activation, we found that both enthalpic and entropic changes were greatly reduced when heat activation was recorded in the presence of Mg^{2+} (Fig. 9 A). At the 10 mM concentration, Mg^{2+} shifted the free energy change associated with heat activation by 2.7 kcal/mol. Accompanying this energetic effect, there was a substantial shift in the temperature activation range at higher Mg^{2+} concentrations. As shown in Fig. 9 B, the half-activation temperature was significantly lowered by 30 mM Mg^{2+}. The large energetic effects on heat activation suggest that Mg^{2+} may directly interact with the heat activation process.

How does Mg^{2+} activate TRPV1?

To understand how Mg^{2+} activates TRPV1, we analyzed our experimental observations using the multi-allosteric model shown in Scheme II (Fig. 1 B). The first step of this analysis was to assign the value of equilibrium constant L for the C↔O transition, which reflects the equilibrium state of the channel pore in the absence of any activation stimulus. Because spontaneous openings of TRPV1 are very rare at room temperature, the equilibrium strongly favors the closed state, i.e., L must be ≪1. Indeed, a small L value was taken in all previous studies of TRPV1 using allosteric modeling (e.g., 2.6×10^{-3} in Jara-Oseguera and Islas, 2013; 4.2×10^{-4} in Matta and Ahern, 2007; 8×10^{-6} in Yao et al., 2010). In the present study, L was taken to be 0.005 (corresponding to a spontaneous open probability of 0.5%) as an upper limit value. A smaller value would better describe the data but does not alter the arguments developed here.

The voltage activation branch

The equilibrium constant of the voltage-dependent transition R↔A in Scheme II (Fig. 1 B) can be expressed as

$$D = \exp\frac{qF\left(V - V_{half}\right)}{RT}.$$

Mg^{2+} may potentially affect the R↔A equilibrium by changing either the gating charge q or the half-activation voltage V_{half}. As shown in Fig. 5, q remained unchanged in the presence of 100 mM Mg^{2+} (0.53 ± 0.03 e_0 vs. 0.56 ± 0.06 e_0). V_{half}, however, shifted substantially to a less depolarized level, from 130.5 ± 1.6 mV to 84.3 ± 1.9 mV. The question is whether this near 50-mV shift in V_{half} is sufficient to substantially affect the C↔O equilibrium to open the channel.

The voltage-dependent activation (Fig. 10 A) is defined as

$$P_o = \frac{L(1 + J_V D)}{1 + D + L(1 + J_V D)}. \quad (3)$$

Using L = 0.005 and the values for D defined by experimentally determined q and V_{half}, the value for the allosteric coupling factor J_V could be determined by fitting

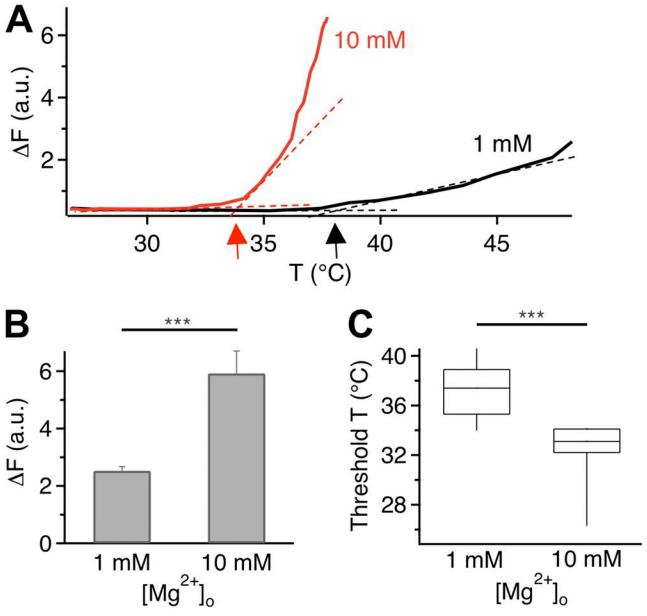

Figure 8. Shift in TRPV1 heat activation measured by fluorescence imaging. (A) Change in fluorescence intensity as a function of temperature in the presence of 1 mM (black) or 10 mM (red) Mg^{2+}. Arrows indicate the activation threshold temperature. (B) Comparison of heat-induced fluorescence increases at two Mg^{2+} concentrations. Error bars indicate ±SEM. (C) Mg^{2+} significantly lowers the activation threshold temperature. ***, P < 0.001; n = 58 (for 1 mM Mg^{2+}) and 28 (for 10 mM Mg^{2+}).

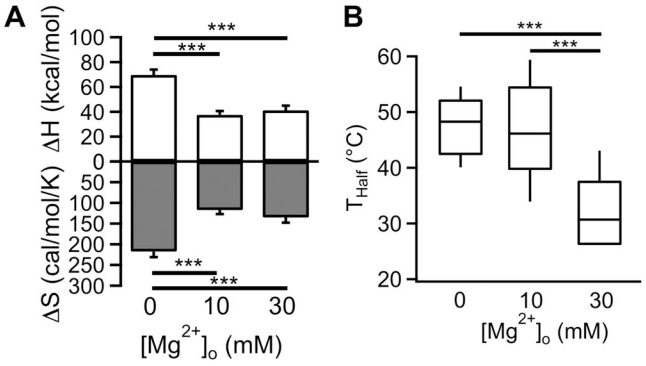

Figure 9. Thermodynamic analysis of Mg^{2+} effects on heat activation. (A) Measured ΔH values (open bars) and ΔS values (shaded bars) from heat-induced currents. Error bars indicate ±SEM. (B) Box-and-whisker plot of the half-activation temperature T_{half} at the corresponding Mg^{2+} concentration. ***, P < 0.001; n = 5–6.

the *G-V* relationship in the absence of Mg^{2+}. A rather small value of $J_V = 7$ best reproduced the observed open probability level and the observed *G-V* relationship. This is anticipated because, in the absence of another stimulus, voltage is a poor activator for TRPV1. Even at +300 mV, when D was ⩾1 and the R↔A equilibrium fully shifted to the right, the channel open probability, $P_o = LJ_V/(1 + LJ_V)$, remained very low in the absence of Mg^{2+} (∼1.7% at +80 mV; Fig. 5 A, left). Because of the small J_V value, a shift of the R↔A equilibrium has a minor influence on channel activation, as can be seen in Fig. 10 A. In the presence of 100 mM Mg^{2+}, the maximum open probability predicted by the model is 3.3% (at 300 mV), much lower than the experimentally determined level, which is 27% at +80 mV and room temperature. Hence, Mg^{2+} can't open the channel through the voltage-dependent branch of Scheme II (Fig. 1 B). The shift in V_{half} observed in the presence of Mg^{2+} can be explained instead by an allosteric coupling of the R↔A equilibrium to the C↔O equilibrium; this will be discussed later in "Energetic effects of heat activation on the voltage and capsaicin branches."

The capsaicin activation branch

As the Mg^{2+} effects on channel activation were observed in the absence of capsaicin, according to the allosteric mechanism of Scheme II (Fig. 1 B), they can't be achieved through the capsaicin activation branch. The observed shift in capsaicin dose–response relationship in the presence of Mg^{2+} is again due to allosteric coupling; this will be discussed later in "Energetic effects of heat activation on the voltage and capsaicin branches."

The heat activation branch

The equilibrium constant C for the heat-dependent transition N↔P is determined by the associated enthalpic and entropic changes:

$$C = \exp\left(-\Delta H/RT + \Delta S/R\right).$$

A consensus from multiple studies of the thermodynamics of TRPV1 gating is that ΔH and ΔS are substantially larger than those observed from most channel gating processes (Voets et al., 2004; Yang et al., 2010; Yao et al., 2010; Cao et al., 2013). In agreement with these previous studies, ΔH and ΔS were estimated in the present study to be 69.7 ± 4.3 kcal/mol and 217.3 ± 13.6 cal/mol/K, respectively (Fig. 9 A). The large ΔH and ΔS values make the N↔P equilibrium extremely temperature-sensitive. When coupled to the C↔O equilibrium, they make the channel activation highly dependent on temperature. The temperature-dependent activation (Fig. 10 B) is defined as

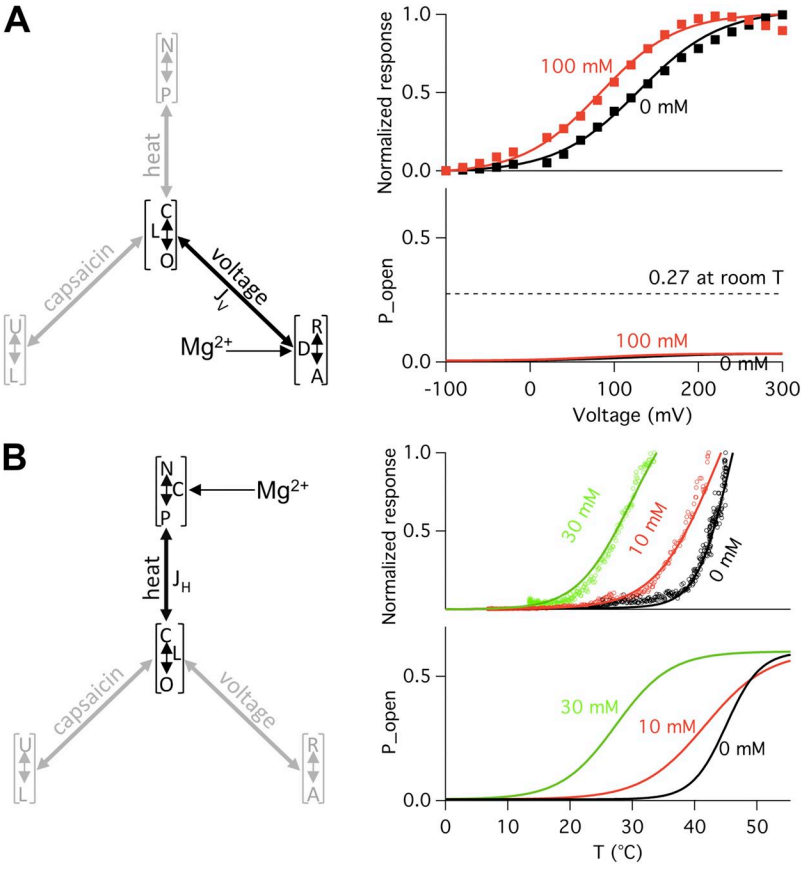

Figure 10. Identification of the Mg^{2+} target in the multi-allosteric TRPV1 gating model. All simulations were generated using values derived from experimental data presented in Figs. 3, 5, 6, and 9, and the following parameters: $L = 0.005$, $J_H = 300$, and $J_V = 7$. (A) Effects of Mg^{2+} on channel open probability through the voltage-dependent branch. (left) The voltage-dependent branch of the gating pyramid, with Mg^{2+} affecting the equilibrium constant D. (right, top) Normalized *P-V* curves in the absence (black curve) or presence (red curve) of 100 mM Mg^{2+}. Superimposed are experimentally determined *G-V* relationships (closed squares). (right, bottom) Predicted channel open probabilities using Eq. 3. The maximal open probability level in the presence of 100 mM Mg^{2+} is significantly lower than the experimental observation (indicated by the broken line), which is ∼27% at +80 mV and room temperature (see Fig. 3 B). (B) Effects of Mg^{2+} on channel open probability through the heat-dependent branch. (right, top) Predicted heat dependence in the absence (black curve) or presence of 10 mM (red curve) or 30 mM (green curve) Mg^{2+}. Superimposed are experimentally determined *I-T* relationships (circles). (right, bottom) Predicted channel open probabilities using Eq. 4.

$$P_o = \frac{L(1 + J_H C)}{1 + C + L(1 + J_H C)}. \quad (4)$$

Because heat can bring the open probability to a high level, J_H must be ⩾1. This can be seen in the reduced Eq. 4 when C ⩾ 1 (a condition reached at elevated temperatures):

$$P_o = \frac{LJ_H}{1 + LJ_H}.$$

Given that $L = 0.005$, to reach an open probability of 50%, J_H needs to be 200; to reach an open probability of 90%, J_H needs to be 1,800. The large J_H value strongly couples the C↔O equilibrium to the N↔P equilibrium, which is expected for a highly temperature-sensitive channel. Because of this strong coupling, it is anticipated that Mg^{2+} can effectively activate the channel by shifting the N↔P equilibrium.

We observed that, in the presence of increasing concentrations of Mg^{2+}, both the values of ΔH and ΔS were substantially reduced (Fig. 9 A), which indicates a reduction of the overall temperature sensitivity. Also noticeable is the substantial shift of the half-activation temperature to lower temperatures (Fig. 9 B), indicating that at room temperature the N↔P equilibrium progressively shifts to the right by Mg^{2+}. We found that both high open probability and left-shifted threshold temperature can be satisfactorily reproduced assuming Mg^{2+} affects only the N↔P equilibrium (Fig. 10 B). This apparently is how Mg^{2+} activates the channel: by shifting the equilibrium of the heat-dependent transition, Mg^{2+} moves the activation range toward room temperature, causing the channel to be heat-activated.

Energetic effects of heat activation on the voltage and capsaicin branches

The preceding discussions demonstrate that potentiation of TRPV1 activation by Mg^{2+} can be explained by a direct effect on the N↔P equilibrium. To conclude the multi-allosteric model analysis, let's consider the energetic effects of Mg^{2+} on the voltage and capsaicin branches of Scheme II (Fig. 1 B). While Mg^{2+} shifts the N↔P equilibrium to activate the channel, the resulted shift of the C↔O equilibrium would also make it easier for capsaicin and voltage to open the channel. The voltage- and capsaicin-dependent activations in the presence of this influence are defined as

$$P_O = \frac{L(1 + J_H C + J_V D + J_H C J_V D J_{VH})}{1 + C + D + J_{VH} CD + L(1 + J_H C + J_V D + J_H C J_V D J_{VH})} \quad (5)$$

and

$$P_O = \frac{L(1 + J_H C + J_C E + J_H C J_C E J_{CH})}{1 + C + E + J_{CH} CE + L(1 + J_H C + J_C E + J_H C J_C E J_{CH})}, \quad (6)$$

respectively. Fig. 11 shows changes in the *G-V* curve (A) and the capsaicin dose–response curve (B), assuming that Mg^{2+} only affects the N↔P equilibrium. Using the same set of parameters that generated the results shown in Fig. 10, Eqs. 5 and 6 predict that Mg^{2+} indeed substantially elevates the open probability upon depolarization (Fig. 11 A) and left-shifts the capsaicin dose–response curve (Fig. 11 B). These simulations demonstrate that voltage- and capsaicin-dependent activations can be adequately altered through allosteric coupling of the Mg^{2+} effects on heat activation.

Divalent cations induce TRPV1 desensitization to heat but not to capsaicin

Thermodynamic analysis suggests that Mg^{2+} activates TRPV1 by potentiating heat activation. If this is true, Mg^{2+} should be able to affect the heat activation process independent of the other stimuli. To directly test this prediction, we replaced Mg^{2+} with Ba^{2+} in our experiments and examined the channel desensitization process. Like Mg^{2+}, Ba^{2+} was found to also strongly potentiate the channel, eliciting an appreciable current at room temperature. As expected, all tested properties of Ba^{2+} potentiation mirrored that of Mg^{2+} (unpublished data). The overall similarity between the effects of Mg^{2+} and Ba^{2+} on TRPV1 indicates that Ba^{2+} potentiates the channel through the same pathway that mediates the Mg^{2+} potentiation effect. We noticed, however, that the Ba^{2+}-elicited macroscopic current was in general much smaller in amplitude compared with that elicited by Mg^{2+}. The observation led us to investigate the desensitization behavior of the channel.

TRPV1 activity is known to undergo rapid desensitization when recorded in intact cells. The process is Ca^{2+}-dependent and is mediated by calmodulin (Numazaki et al., 2003; Rosenbaum et al., 2004; Lishko et al., 2007; Grycova et al., 2008; Lau et al., 2012), phosphatase (Docherty et al., 1996; Mohapatra and Nau, 2005), and other factors (Lukacs et al., 2007; Ufret-Vincenty et al., 2011; Cao et al., 2013). Removal of Ca^{2+} prevented this rapid desensitization process. However, removing Ca^{2+} revealed a slower, Ca^{2+}-independent desensitization process in heat-activated TRPV1 channels, as can be seen in the current traces shown in Fig. 7 A. Interestingly, Mg^{2+}- and Ba^{2+}-induced TRPV1 activation also exhibited Ca^{2+}-independent desensitization. Hints of a slow desensitization process can be seen in the representative fluorescence recording shown in Fig. 2 B and current recording shown in Fig. 3 A. Ba^{2+}-induced channel desensitization was much more rapid than Mg^{2+}-induced desensitization. An example demonstrating the time course of Ba^{2+}-elicited current is shown in Fig. 12 A,

where a rapid decline in current amplitude is seen with a dominant time constant of 5.8 ± 1.0 s (n = 4). The Mg^{2+}-elicited current declined with a dominant time constant of 84.5 ± 17.9 s (n = 3), more than 10 times larger than that of Ba^{2+}-induced desensitization. It is hence most likely that rapid desensitization substantially diminished the Ba^{2+}-elicited current, making the Ba^{2+} potentiating effect appeared to be less strong than that of Mg^{2+}.

To investigate the underlying mechanism for the divalent cation-induced Ca^{2+}-independent desensitization process, we designed a two-step protocol, as shown in Fig. 12 B. A short temperature ramp was first delivered to induce heat activation in cell-free inside-out patches in a Ca^{2+}-free solution. After closing the channels by cooling, the same membrane patch was challenged by 3 µM capsaicin to induce agonist activation. In the absence of divalent cation, temperature-induced current kept increasing in amplitude up to 50°C, yielding a current comparable in size to that induced by capsaicin (Fig. 12, B and D). However, for patches exposed to Ba^{2+} before and during recording, heat could no longer effectively activate the channels, though the capsaicin-induced current remained (Fig. 12, C and D). The lack of heat-induced current suggests that during the extended presence of Ba^{2+}, the heat activation machinery was mostly desensitized. Indeed, as can be seen in Fig. 7 A, desensitization of heat-activated channel current becomes more prominent and occurs at progressively lower temperatures in the presence of increasing concentrations of Mg^{2+}. Desensitization of the heat activation machinery, however, did not prevent capsaicin-induced activation (Fig. 12 E), which is consistent with the notion that capsaicin activation and heat activation use separate pathways. These results further confirmed that Mg^{2+} and Ba^{2+} potentiate TRPV1 by selectively interacting with the heat activation pathway.

DISCUSSION

Our data demonstrate that the divalent cations Mg^{2+} and Ba^{2+} dose-dependently potentiate TRPV1 activation. This gating effect is partially covered by an inhibitory effect on the single-channel conductance. Adjusting for the conductance difference revealed strong potentiation of TRPV1 gating by Mg^{2+} that brings the channel open probability to ∼25% at room temperature. The substantial effect on channel gating, observed from both current and fluorescence recordings, are in close agreement with several previous studies using divalent and multivalent cations (Ahern et al., 2005, 2006; Tousova et al., 2005; Riera et al., 2007; Ohta et al., 2008; Luebbert et al., 2010), with minor quantitative differences that are accountable to variations in experimental conditions. For example, the apparently lower EC_{50} value for Mg^{2+} in a previous study (Riera et al., 2007) might be due to a combination of differences in channel homologues (mouse vs. human), Ca^{2+} indicator dye (Fluo-4 vs. Fura-2), and perhaps the use of SO_4^{2-} instead of Cl^- as the counter ion in the previous study; indeed, at the same concentration (10 mM), $NiSO_4$ was found to be more effective than $NiCl_2$ in potentiating

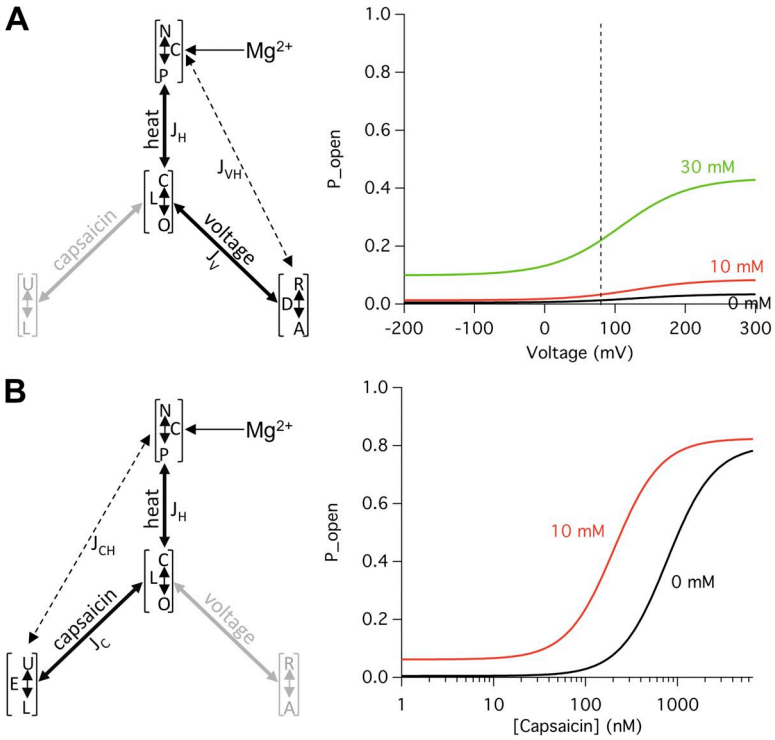

Figure 11. Mg^{2+} potentiation of heat activation can substantially affect voltage- and capsaicin-dependent activation. All simulations were generated using values derived from experimental data presented in Figs. 3, 5, 6, and 9, and the following parameters: L = 0.005, J_H = 300, J_V = 7, J_C = 800, J_{VH} = 1, and J_{CH} = 1. (A) Mg^{2+} effects on voltage-dependent activation. (left) The dual-allosteric model containing the heat and voltage branches, with Mg^{2+} affecting the equilibrium constant C. (right) Predicted voltage-dependent activation using Eq. 5. The broken line indicates the position of +80 mV. (B) Mg^{2+} effects on capsaicin-dependent activation. (left) The dual-allosteric model containing the heat and capsaicin branches, with Mg^{2+} affecting the equilibrium constant C. (right) Predicted capsaicin dose–response curves using Eq. 6.

TRPV1 (Luebbert et al., 2010). More importantly, our present study suggests that potentiation of TRPV1 by Mg^{2+} and Ba^{2+} is achieved predominantly by lowing the channel's heat activation threshold so that the channel starts to be heat-activated at room temperature.

Although phenomenally divalent cations shift the temperature range at which heat activation occurs, quantitative comparison of the energetic effects of Mg^{2+} on each activation pathway suggests that mechanistically divalent cations potentiate TRPV1 by reducing the energy barrier for heat activation. Both the enthalpic change and the entropic change associated with heat activation are substantially lowered in the presence of Mg^{2+}. As a result, it requires less thermal energy to drive heat activation. Thermodynamic studies showed that heat activation of thermo-TRP channels is associated with large changes in enthalpy and entropy (Voets et al., 2004; Yang et al., 2010; Yao et al., 2010). The magnitude of these changes indicates a substantial conformational change in the channel protein (Clapham and Miller, 2011). Although the nature of this heat-induced conformational change remains elusive, its presence could be detected directly with fluorophores attached to the pore turret (Yang et al., 2010). Interestingly, while fluorophores on the pore turret reported a conformational change during heat-dependent activation, there is no evidence of a conformational change at the same position during capsaicin- or voltage-dependent activation. The large change in thermodynamic properties by Mg^{2+} observed in the present study is consistent with these earlier findings, suggesting that the presence of Mg^{2+} and Ba^{2+} may promote the heat activation conformational change through which it exerts potentiation effects on TRPV1 activation. It is important to note that changes in thermodynamic properties may arise from a change in either the equilibrium constant C of the N↔P transition (which may be considered to represent the "heat sensor") or the coupling factor J_H. Measurements in the present study could not distinguish between these two alternatives. Future experiments are required to establish whether Mg^{2+} directly affects movement of the heat sensor or the structure that couples the heat sensor to the activation gate. For this reason, in this paper we restrict our discussion to distinguishing between heat, voltage, and capsaicin "activation pathways."

TRPV1 is a polymodal cellular sensor for voltage, capsaicin, and heat (Tominaga et al., 1998). These stimuli likely work through separate activation pathways (Jordt et al., 2000; Matta and Ahern, 2007; Grandl et al., 2010; Yang et al., 2010; Cui et al., 2012) but synergistically activate the channel. As a result of functional coupling, experimental perturbation to one modality would allosterically affect the channel's response to other modalities. While mutagenesis studies in recent years have yielded several important observations that may shed new light on the structural basis for heat activation, it is important to realize that, because of functional couplings between different activation pathways, almost every perturbation to channel gating may manifest in a change of the channel's response to other stimuli (Brauchi et al., 2004; Latorre et al., 2007). Current potentiation by divalent cations demonstrates again the synergistic nature of activating a polymodal channel like TRPV1. It underlines the need to distinguish direct

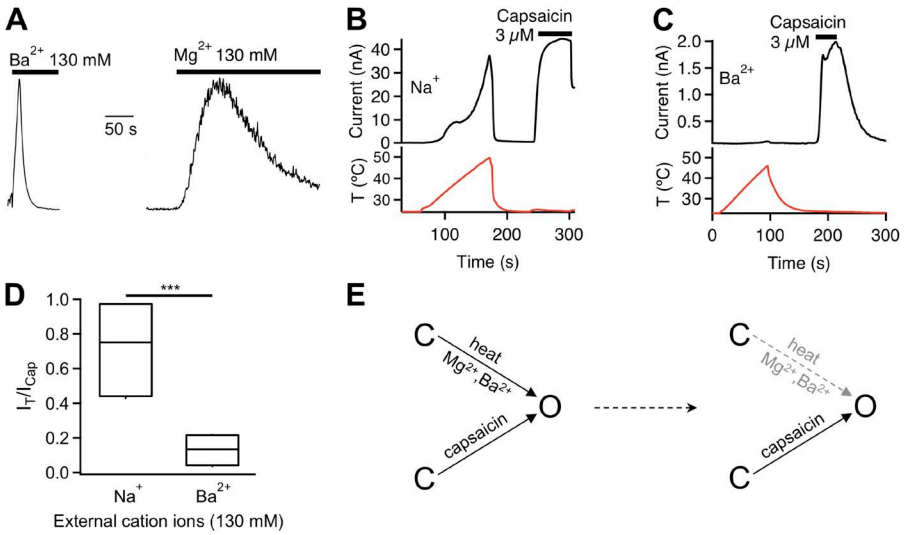

Figure 12. Divalent cations induce desensitization of the heat activation pathway but not the capsaicin activation pathway. (A) Normalized current traces demonstrating transient activation of TRPV1 by 130 mM extracellular Ba^{2+} (left) or Mg^{2+} (right), followed by rapid desensitization. (B) Time course of whole-cell current (black trace) at +80 mV evoked first by heat (red trace below current trace) and subsequently by 3 µM capsaicin (black bar above current trace). (C) Same as for B, but in the presence of 130 mM Ba^{2+} instead of Na^+. (D) Box-and-whisker plot of the ratio between current evoked by raising temperature to 45°C and current evoked by 3 µM capsaicin in a bath solution containing the indicated cations. ***, $P < 0.001$; $n = 4–5$. (E) Schematic gating diagram illustrating the separation of the capsaicin activation pathway and the heat–Mg^{2+}–Ba^{2+} pathway (left). In the presence of Mg^{2+} or Ba^{2+}, the heat–Mg^{2+}–Ba^{2+} pathway is desensitized over time but the capsaicin activation remains functional (right).

versus indirect interactions and highlights the advantage of modality-specific perturbation methods in mechanistic investigations.

Desensitization of the TRPV1 gating machinery

TRPV1 exhibits complex desensitization properties. The dominant and rapid desensitization process is found to be Ca^{2+}-dependent (Docherty et al., 1996; Koplas et al., 1997). It is shown that Ca^{2+}-dependent desensitization is partly caused by channel modulation by Ca^{2+}-calmodulin, which binds to two intracellular sites, one in the channel's C-terminal region and the other in the Ankyrin-like repeat domains of the N-terminal region (Numazaki et al., 2003; Rosenbaum et al., 2004; Lishko et al., 2007; Grycova et al., 2008; Lau et al., 2012). Desensitization occurs when Ca^{2+} enters the cell through activated TRPV1 channels and activates calmodulin. This Ca^{2+}-dependent desensitization process is often observed in experiments using whole-cell recordings but is also observed in cell-free patch recordings when Ca^{2+} is present. It plays a major role in channel down-regulation upon prolonged or repetitive stimuli under physiological or pathological conditions (for review see Vyklický et al., 2008).

Preventing Ca^{2+}-dependent desensitization by excluding Ca^{2+} from experimental solutions reveals the existence of other types of desensitization. For example, repetitive or extended heating to high temperatures leads to current decline in TRPV1 (Tominaga et al., 1998), which is demonstrated in Fig. 7 A of this paper. We observed a similar Ca^{2+}-independent desensitization process in Mg^{2+}-and Ba^{2+}-induced currents. Because Mg^{2+} and Ba^{2+} shift the heat activation process, it is likely that desensitization of TRPV1 after heat or divalent cation activation reflects a common gating process. This is confirmed by the observation that Mg^{2+}/Ba^{2+}-desensitized channels can no longer be heat-activated. The finding that capsaicin remains effective in activating TRPV1 after Mg^{2+}- or Ba^{2+}-induced desensitization is fully consistent with this idea and confirms the separation of the capsaicin and heat activation pathways. More importantly, the observation suggests that heat- and divalent cation–induced desensitization does not involve the closure of a distinct inactivation gate. Instead, it is an earlier step of the heat activation process that has become desensitized to heat and divalent cations so that it can no longer sustain the opening of the activation gate.

Several molecular events are known in various channel types to terminate ion flux upon extended activation. Two inactivation processes occur in *Shaker* potassium channels: the N-type inactivation involves physically plugging the open pore with an "inactivation ball" peptide (Hoshi et al., 1990; Zagotta et al., 1990), whereas the C-type inactivation arises from conformational changes in the outer mouth of the pore (Choi et al., 1991; Yellen et al., 1994; Baukrowitz and Yellen, 1995, 1996; Liu et al., 1996). It is noted that for both inactivation processes a distinct "gate" is shut to prevent ion flux even though the main activation gate remains open. Ligand-gated channels terminate ion flux in the extended presence of ligand molecules through a desensitization process that recloses the same gate that is opened during activation. In the glutamate receptor this is achieved by relaxing a part of the gating machinery that experiences a strain caused by the activation stimulus (Sun et al., 2002). Hyperpolarization-activated cyclic nucleotide-modulated (HCN) channels desensitize to voltage through a slippage in the coupling between the voltage sensor and the activation gate that relieves the strain in the gating machinery (Shin et al., 2004). An important distinction between the inactivation mechanism and the desensitization mechanism is that an inactivated channel cannot reopen before the inactivation gate opens again, whereas a desensitized channel can be opened by a stimulus that avoids the desensitized gating machinery and works through a separate pathway. In the present study we present direct evidence in support of this prediction. Because Ca^{2+}-independent desensitization of TRPV1 does not prevent subsequent capsaicin activation, it is most likely not caused by a distinct inactivation gate, but rather by closing the main activation gate that is formed by the lower part of the S6 segments (Salazar et al., 2009). The desensitization process may occur locally to the same channel structure that undergoes heat-induced activation conformational changes, leading to the closure of the activation gate.

We are grateful to our laboratory members for assistance and helpful discussion throughout the course of this study, Drs. William N. Zagotta and Frank Horrigan for advice on the allosteric mechanism, and Drs. Jon Sack and Vladimir Yarov-Yarovoy for critical reading of the manuscript.

This work was supported by a grant from National Institutes of Health (R01NS072377) and a UC Davis Health System Research Award (to J. Zheng); grants from the Ministry of Education of China 111 Project (B07001), the Ministry of Science and Technology of China (2013CB531302), and the National Science Foundation of China (81221002; to K.W. Wang); an Australian National Health and Medical Research Council fellowship (APP1035102 to L. Ma); and an American Heart Association predoctoral fellowship (10PRE4170142 to F. Yang).

The authors have no conflicting financial interests.

Sharona E. Gordon served as editor.

Submitted: 9 May 2013
Accepted: 22 November 2013

REFERENCES

Ahern, G.P., I.M. Brooks, R.L. Miyares, and X.B. Wang. 2005. Extracellular cations sensitize and gate capsaicin receptor TRPV1 modulating pain signaling. *J. Neurosci.* 25:5109–5116. http://dx.doi.org/10.1523/JNEUROSCI.0237-05.2005

Ahern, G.P., X. Wang, and R.L. Miyares. 2006. Polyamines are potent ligands for the capsaicin receptor TRPV1. *J. Biol. Chem.* 281:8991–8995. http://dx.doi.org/10.1074/jbc.M513429200

Baukrowitz, T., and G. Yellen. 1995. Modulation of K+ current by frequency and external [K+]: a tale of two inactivation mechanisms. *Neuron.* 15:951–960. http://dx.doi.org/10.1016/0896-6273(95)90185-X

Baukrowitz, T., and G. Yellen. 1996. Use-dependent blockers and exit rate of the last ion from the multi-ion pore of a K+ channel. *Science.* 271:653–656. http://dx.doi.org/10.1126/science.271.5249.653

Brauchi, S., P. Orio, and R. Latorre. 2004. Clues to understanding cold sensation: thermodynamics and electrophysiological analysis of the cold receptor TRPM8. *Proc. Natl. Acad. Sci. USA.* 101:15494–15499. http://dx.doi.org/10.1073/pnas.0406773101

Cao, E., J.F. Cordero-Morales, B. Liu, F. Qin, and D. Julius. 2013. TRPV1 channels are intrinsically heat sensitive and negatively regulated by phosphoinositide lipids. *Neuron.* 77:667–679. http://dx.doi.org/10.1016/j.neuron.2012.12.016

Caterina, M.J., M.A. Schumacher, M. Tominaga, T.A. Rosen, J.D. Levine, and D. Julius. 1997. The capsaicin receptor: a heat-activated ion channel in the pain pathway. *Nature.* 389:816–824. http://dx.doi.org/10.1038/39807

Cheng, W., F. Yang, C.L. Takanishi, and J. Zheng. 2007. Thermosensitive TRPV channel subunits coassemble into heteromeric channels with intermediate conductance and gating properties. *J. Gen. Physiol.* 129:191–207. http://dx.doi.org/10.1085/jgp.200709731

Choi, K.L., R.W. Aldrich, and G. Yellen. 1991. Tetraethylammonium blockade distinguishes two inactivation mechanisms in voltage-activated K+ channels. *Proc. Natl. Acad. Sci. USA.* 88:5092–5095. http://dx.doi.org/10.1073/pnas.88.12.5092

Chuang, H.H., E.D. Prescott, H. Kong, S. Shields, S.E. Jordt, A.I. Basbaum, M.V. Chao, and D. Julius. 2001. Bradykinin and nerve growth factor release the capsaicin receptor from PtdIns(4,5)P2-mediated inhibition. *Nature.* 411:957–962. http://dx.doi.org/10.1038/35082088

Clapham, D.E. 2003. TRP channels as cellular sensors. *Nature.* 426:517–524. http://dx.doi.org/10.1038/nature02196

Clapham, D.E., and C. Miller. 2011. A thermodynamic framework for understanding temperature sensing by transient receptor potential (TRP) channels. *Proc. Natl. Acad. Sci. USA.* 108:19492–19497. http://dx.doi.org/10.1073/pnas.1117485108

Cui, Y., F. Yang, X. Cao, V. Yarov-Yarovoy, K. Wang, and J. Zheng. 2012. Selective disruption of high sensitivity heat activation but not capsaicin activation of TRPV1 channels by pore turret mutations. *J. Gen. Physiol.* 139:273–283. http://dx.doi.org/10.1085/jgp.201110724

Dhaka, A., V. Uzzell, A.E. Dubin, J. Mathur, M. Petrus, M. Bandell, and A. Patapoutian. 2009. TRPV1 is activated by both acidic and basic pH. *J. Neurosci.* 29:153–158. http://dx.doi.org/10.1523/JNEUROSCI.4901-08.2009

Docherty, R.J., J.C. Yeats, S. Bevan, and H.W. Boddeke. 1996. Inhibition of calcineurin inhibits the desensitization of capsaicin-evoked currents in cultured dorsal root ganglion neurones from adult rats. *Pflugers Arch.* 431:828–837.

Gee, K.R., K.A. Brown, W.N. Chen, J. Bishop-Stewart, D. Gray, and I. Johnson. 2000. Chemical and physiological characterization of fluo-4 Ca(2+)-indicator dyes. *Cell Calcium.* 27:97–106. http://dx.doi.org/10.1054/ceca.1999.0095

Grandl, J., S.E. Kim, V. Uzzell, B. Bursulaya, M. Petrus, M. Bandell, and A. Patapoutian. 2010. Temperature-induced opening of TRPV1 ion channel is stabilized by the pore domain. *Nat. Neurosci.* 13:708–714. http://dx.doi.org/10.1038/nn.2552

Grycova, L., Z. Lansky, E. Friedlova, V. Obsilova, H. Janouskova, T. Obsil, and J. Teisinger. 2008. Ionic interactions are essential for TRPV1 C-terminus binding to calmodulin. *Biochem. Biophys. Res. Commun.* 375:680–683. http://dx.doi.org/10.1016/j.bbrc.2008.08.094

Horrigan, F.T., and R.W. Aldrich. 1999. Allosteric voltage gating of potassium channels II. Mslo channel gating charge movement in the absence of Ca(2+). *J. Gen. Physiol.* 114:305–336. http://dx.doi.org/10.1085/jgp.114.2.305

Horrigan, F.T., and R.W. Aldrich. 2002. Coupling between voltage sensor activation, Ca2+ binding and channel opening in large conductance (BK) potassium channels. *J. Gen. Physiol.* 120:267–305. http://dx.doi.org/10.1085/jgp.20028605

Horrigan, F.T., J. Cui, and R.W. Aldrich. 1999. Allosteric voltage gating of potassium channels I. Mslo ionic currents in the absence of Ca(2+). *J. Gen. Physiol.* 114:277–304. http://dx.doi.org/10.1085/jgp.114.2.277

Hoshi, T., W.N. Zagotta, and R.W. Aldrich. 1990. Biophysical and molecular mechanisms of Shaker potassium channel inactivation. *Science.* 250:533–538. http://dx.doi.org/10.1126/science.2122519

Jahnel, R., M. Dreger, C. Gillen, O. Bender, J. Kurreck, and F. Hucho. 2001. Biochemical characterization of the vanilloid receptor 1 expressed in a dorsal root ganglia derived cell line. *Eur. J. Biochem.* 268:5489–5496. http://dx.doi.org/10.1046/j.1432-1033.2001.02500.x

Jara-Oseguera, A., and L.D. Islas. 2013. The role of allosteric coupling on thermal activation of thermo-TRP channels. *Biophys. J.* 104:2160–2169. http://dx.doi.org/10.1016/j.bpj.2013.03.055

Jordt, S.E., and D. Julius. 2002. Molecular basis for species-specific sensitivity to "hot" chili peppers. *Cell.* 108:421–430. http://dx.doi.org/10.1016/S0092-8674(02)00637-2

Jordt, S.E., M. Tominaga, and D. Julius. 2000. Acid potentiation of the capsaicin receptor determined by a key extracellular site. *Proc. Natl. Acad. Sci. USA.* 97:8134–8139. http://dx.doi.org/10.1073/pnas.100129497

Kedei, N., T. Szabo, J.D. Lile, J.J. Treanor, Z. Olah, M.J. Iadarola, and P.M. Blumberg. 2001. Analysis of the native quaternary structure of vanilloid receptor 1. *J. Biol. Chem.* 276:28613–28619. http://dx.doi.org/10.1074/jbc.M103272200

Koplas, P.A., R.L. Rosenberg, and G.S. Oxford. 1997. The role of calcium in the desensitization of capsaicin responses in rat dorsal root ganglion neurons. *J. Neurosci.* 17:3525–3537.

Kuzhikandathil, E.V., H. Wang, T. Szabo, N. Morozova, P.M. Blumberg, and G.S. Oxford. 2001. Functional analysis of capsaicin receptor (vanilloid receptor subtype 1) multimerization and agonist responsiveness using a dominant negative mutation. *J. Neurosci.* 21:8697–8706.

Latorre, R., S. Brauchi, G. Orta, C. Zaelzer, and G. Vargas. 2007. ThermoTRP channels as modular proteins with allosteric gating. *Cell Calcium.* 42:427–438. http://dx.doi.org/10.1016/j.ceca.2007.04.004

Lau, S.Y., E. Procko, and R. Gaudet. 2012. Distinct properties of Ca2+-calmodulin binding to N- and C-terminal regulatory regions of the TRPV1 channel. *J. Gen. Physiol.* 140:541–555. http://dx.doi.org/10.1085/jgp.201210810

Lishko, P.V., E. Procko, X. Jin, C.B. Phelps, and R. Gaudet. 2007. The ankyrin repeats of TRPV1 bind multiple ligands and modulate channel sensitivity. *Neuron.* 54:905–918. http://dx.doi.org/10.1016/j.neuron.2007.05.027

Liu, Y., M.E. Jurman, and G. Yellen. 1996. Dynamic rearrangement of the outer mouth of a K+ channel during gating. *Neuron.* 16:859–867. http://dx.doi.org/10.1016/S0896-6273(00)80106-3

Luebbert, M., D. Radtke, R. Wodarski, N. Damann, H. Hatt, and C.H. Wetzel. 2010. Direct activation of transient receptor potential V1 by nickel ions. *Pflugers Arch.* 459:737–750. http://dx.doi.org/10.1007/s00424-009-0782-8

Lukacs, V., B. Thyagarajan, P. Varnai, A. Balla, T. Balla, and T. Rohacs. 2007. Dual regulation of TRPV1 by phosphoinositides. *J. Neurosci.* 27:7070–7080. http://dx.doi.org/10.1523/JNEUROSCI.1866-07.2007

Matta, J.A., and G.P. Ahern. 2007. Voltage is a partial activator of rat thermosensitive TRP channels. *J. Physiol.* 585:469–482. http://dx.doi.org/10.1113/jphysiol.2007.144287

Minta, A., J.P. Kao, and R.Y. Tsien. 1989. Fluorescent indicators for cytosolic calcium based on rhodamine and fluorescein chromophores. *J. Biol. Chem.* 264:8171–8178.

Mohapatra, D.P., and C. Nau. 2005. Regulation of Ca2+-dependent desensitization in the vanilloid receptor TRPV1 by calcineurin and cAMP-dependent protein kinase. *J. Biol. Chem.* 280:13424–13432. http://dx.doi.org/10.1074/jbc.M410917200

Moiseenkova-Bell, V.Y., L.A. Stanciu, I.I. Serysheva, B.J. Tobe, and T.G. Wensel. 2008. Structure of TRPV1 channel revealed by electron cryomicroscopy. *Proc. Natl. Acad. Sci. USA.* 105:7451–7455. http://dx.doi.org/10.1073/pnas.0711835105

Numazaki, M., T. Tominaga, K. Takeuchi, N. Murayama, H. Toyooka, and M. Tominaga. 2003. Structural determinant of TRPV1 desensitization interacts with calmodulin. *Proc. Natl. Acad. Sci. USA.* 100:8002–8006. http://dx.doi.org/10.1073/pnas.1337252100

Ohta, T., T. Imagawa, and S. Ito. 2008. Novel gating and sensitizing mechanism of capsaicin receptor (TRPV1): tonic inhibitory regulation of extracellular sodium through the external protonation sites on TRPV1. *J. Biol. Chem.* 283:9377–9387. http://dx.doi.org/10.1074/jbc.M709377200

Premkumar, L.S., and G.P. Ahern. 2000. Induction of vanilloid receptor channel activity by protein kinase C. *Nature.* 408:985–990. http://dx.doi.org/10.1038/35050121

Riera, C.E., H. Vogel, S.A. Simon, and J. le Coutre. 2007. Artificial sweeteners and salts producing a metallic taste sensation activate TRPV1 receptors. *Am. J. Physiol. Regul. Integr. Comp. Physiol.* 293:R626–R634. http://dx.doi.org/10.1152/ajpregu.00286.2007

Rosenbaum, T., A. Gordon-Shaag, M. Munari, and S.E. Gordon. 2004. Ca2+/calmodulin modulates TRPV1 activation by capsaicin. *J. Gen. Physiol.* 123:53–62. http://dx.doi.org/10.1085/jgp.200308906

Salazar, H., A. Jara-Oseguera, E. Hernández-García, I. Llorente, I.I. Arias-Olguín, M. Soriano-García, L.D. Islas, and T. Rosenbaum. 2009. Structural determinants of gating in the TRPV1 channel. *Nat. Struct. Mol. Biol.* 16:704–710. http://dx.doi.org/10.1038/nsmb.1633

Samways, D.S., and T.M. Egan. 2011. Calcium-dependent decrease in the single-channel conductance of TRPV1. *Pflugers Arch.* 462:681–691. http://dx.doi.org/10.1007/s00424-011-1013-7

Shin, K.S., C. Maertens, C. Proenza, B.S. Rothberg, and G. Yellen. 2004. Inactivation in HCN channels results from reclosure of the activation gate: desensitization to voltage. *Neuron.* 41:737–744. http://dx.doi.org/10.1016/S0896-6273(04)00083-2

Sigworth, F.J. 1980. The variance of sodium current fluctuations at the node of Ranvier. *J. Physiol.* 307:97–129.

Stein, A.T., C.A. Ufret-Vincenty, L. Hua, L.F. Santana, and S.E. Gordon. 2006. Phosphoinositide 3-kinase binds to TRPV1 and mediates NGF-stimulated TRPV1 trafficking to the plasma membrane. *J. Gen. Physiol.* 128:509–522. http://dx.doi.org/10.1085/jgp.200609576

Sun, Y., R. Olson, M. Horning, N. Armstrong, M. Mayer, and E. Gouaux. 2002. Mechanism of glutamate receptor desensitization. *Nature.* 417:245–253. http://dx.doi.org/10.1038/417245a

Tominaga, M., M.J. Caterina, A.B. Malmberg, T.A. Rosen, H. Gilbert, K. Skinner, B.E. Raumann, A.I. Basbaum, and D. Julius. 1998. The cloned capsaicin receptor integrates multiple pain-producingstimuli. *Neuron.* 21:531–543. http://dx.doi.org/10.1016/S0896-6273(00)80564-4

Tousova, K., L. Vyklicky, K. Susankova, J. Benedikt, and V. Vlachova. 2005. Gadolinium activates and sensitizes the vanilloid receptor TRPV1 through the external protonation sites. *Mol. Cell. Neurosci.* 30:207–217. http://dx.doi.org/10.1016/j.mcn.2005.07.004

Ufret-Vincenty, C.A., R.M. Klein, L. Hua, J. Angueyra, and S.E. Gordon. 2011. Localization of the PIP2 sensor of TRPV1 ion channels. *J. Biol. Chem.* 286:9688–9698. http://dx.doi.org/10.1074/jbc.M110.192526

Voets, T., G. Droogmans, U. Wissenbach, A. Janssens, V. Flockerzi, and B. Nilius. 2004. The principle of temperature-dependent gating in cold- and heat-sensitive TRP channels. *Nature.* 430:748–754. http://dx.doi.org/10.1038/nature02732

Vyklický, L., K. Nováková-Tousová, J. Benedikt, A. Samad, F. Touska, and V. Vlachová. 2008. Calcium-dependent desensitization of vanilloid receptor TRPV1: a mechanism possibly involved in analgesia induced by topical application of capsaicin. *Physiol. Res.* 57(Suppl 3):S59–S68.

Wang, S., K. Poon, R.E. Oswald, and H.H. Chuang. 2010. Distinct modulations of human capsaicin receptor by protons and magnesium through different domains. *J. Biol. Chem.* 285:11547–11556. http://dx.doi.org/10.1074/jbc.M109.058727

Wu, L.J., T.B. Sweet, and D.E. Clapham. 2010. International Union of Basic and Clinical Pharmacology. LXXVI. Current progress in the mammalian TRP ion channel family. *Pharmacol. Rev.* 62:381–404. http://dx.doi.org/10.1124/pr.110.002725

Yang, F., Y. Cui, K. Wang, and J. Zheng. 2010. Thermosensitive TRP channel pore turret is part of the temperature activation pathway. *Proc. Natl. Acad. Sci. USA.* 107:7083–7088. http://dx.doi.org/10.1073/pnas.1000357107

Yang, F., L. Ma, X. Cao, K. Wang, and J. Zheng. 2014. Divalent cations activate TRPV1 through promoting conformational change of the extracellular region. *J. Gen. Physiol.* 143:91–103.

Yao, J., B. Liu, and F. Qin. 2010. Kinetic and energetic analysis of thermally activated TRPV1 channels. *Biophys. J.* 99:1743–1753. http://dx.doi.org/10.1016/j.bpj.2010.07.022

Yellen, G., D. Sodickson, T.Y. Chen, and M.E. Jurman. 1994. An engineered cysteine in the external mouth of a K+ channel allows inactivation to be modulated by metal binding. *Biophys. J.* 66:1068–1075. http://dx.doi.org/10.1016/S0006-3495(94)80888-4

Zagotta, W.N., T. Hoshi, and R.W. Aldrich. 1990. Restoration of inactivation in mutants of Shaker potassium channels by a peptide derived from ShB. *Science.* 250:568–571. http://dx.doi.org/10.1126/science.2122520

Zheng, J. 2013. Molecular mechanism of TRP channels. *Compr. Physiol.* 3:221–242.